Pergamon

0301-9322(94)00061-1

Int. J. Multiphase Flow Vol. 21, No. 2, pp. 137–149, 1995

0301-9322/95 $9.50 + 0.00

THE DISTRIBUTION OF DROP SIZE AND VELOCITY IN GAS–LIQUID ANNULAR FLOW

LARRY B. FORE and ABRAHAM E. DUKLER†

Department of Chemical Engineering, University of Houston, Houston, TX 77204, U.S.A.

(Received 19 May 1994; in revised form 25 July 1994)

Abstract—An experimental study of the droplet size and velocity distributions in gas–liquid annular upflow is reported for a 50.8 mm i.d. vertical tube. Included are the effects of liquid viscosity and the radial variation of drop size and velocity. Additional measurements of the centerline gas velocity are used to estimate the gas–droplet slip ratio. The drop size distributions exhibit a bimodal nature, discounting the use of previously suggested functions for their description. Mean drop sizes are observed to increase with liquid flow rate and viscosity. On average, droplets at the tube centerline are observed to travel at 80% of the local gas velocity.

Key Words: two-phase flow, annular flow, droplet entrainment, droplet sizes

INTRODUCTION

During the simultaneous upflow of gas and liquid in a tube, several flow patterns can exist, depending on the input flow rates and physical properties. The annular flow pattern is characterized by the flow of a thin, wavy liquid film along the inner wall, with a core of gas flowing in the center. At gas velocities slightly above the flooding condition, film-churning occurs, with the liquid film at any position moving up or down locally. As the gas velocity is increased, large disturbance waves appear (Hall-Taylor *et al.* 1963; Nedderman & Shearer 1963). Above a critical liquid flow rate, droplets form from the disturbance waves, accelerate in the gas core and deposit back onto the film. The droplets represent a larger interfacial transfer area than the liquid film and thus can dominate heat and mass transport between the phases. System pressure drop is increased by droplet acceleration in the gas core and depositing droplets contribute to corrosion by increasing local wall friction.

Due to the variety of situations under which annular flow occurs, from power generation systems to gas–liquid contactors and the effects mentioned above, there has been significant interest in the measurement and prediction of the characteristics of the dispersed droplets. Several techniques have been used to measure the drop size distributions in annular flow. Cousins & Hewitt (1968), among others, utilized photography. Wicks & Dukler (1966) and Tatterson *et al.* (1977) used electrical contact methods. The laser-diffraction technique of Swithenbank *et al.* (1976) was employed by Azzopardi *et al.* (1978), and in a number of subsequent studies (Azzopardi *et al.* 1980; Azzopardi 1985; Jepson *et al.* 1989, 1990; Azzopardi *et al.* 1991). The laser-grating technique of Semiat & Dukler (1981) was employed by Lopes & Dukler (1986, 1987) to obtain simultaneous drop sizes and velocities. Recently, Azzopardi & Teixeira (1992) used the phase-Doppler technique developed by Bachalo (1980) to measure drop sizes and velocities in annular flow.

There has been some disparity between measurements obtained with the techniques listed above. One source of disagreement is an inherent limit in the range of measurable droplet sizes. The range of drop sizes in gas–liquid annular flow extends from a few microns to several millimeters but, each of these techniques is limited, usually through the experimental set-up to either the upper or lower end of the size spectrum. Photography is limited to droplets larger than about 100–200 μm, as are electrical contact methods. The laser-diffraction technique utilizes a special optical detector to measure the diffraction pattern produced by interference between the droplet spray and a

†Deceased.

collimated laser beam. The size and orientation of the detector determines the upper and lower limits of the size distribution. Similarly, the upper and lower limits of the size distribution are determined by the placement of an off-angle photodetector in the phase-Doppler technique. The laser-grating technique applied by Lopes & Dukler (1986) was limited to drop sizes above 100 μm by the size of an optic that measured the droplet passage time. Both the phase-Doppler and laser-grating techniques are limited in accuracy for large, distorted drops, since the former measures radius of curvature while the latter measures the length of one major axis.

In addition to dynamic range limitations of the various drop-sizing techniques, there has always been the problem of obtaining optical access to the gas–droplet core. In the more recent work, annular flow measurements with the laser-diffraction and phase-Doppler techniques required removal of the liquid film prior to drop sizing. Lopes & Dukler (1986) retained the liquid film, accessing the core region with protruding glass rods. Of these three methods, the laser-grating and phase-Doppler techniques produce local measurements of drop size and velocity, while the laser diffraction technique produces the size distribution, averaged over the tube cross-section.

Significant improvements have been made to the Lopes & Dukler (1986) technique in the work presented here. The lower limit of size resolution has been extended to less than 10 μm, so that the measurable range now includes nearly all of the drops in annular flow. This improved laser-grating technique has been used to measure simultaneous drop size and velocity distributions for two gas–liquid systems over a range of operating conditions. This paper presents these measurements and several new implications associated with them.

EXPERIMENTAL

Flow loop

The flow loop used in this study is depicted in figure 1. The test section was a vertical column, constructed of 50.8 mm i.d. clear acrylic tubing, configured for cocurrent upflow of gas and liquid

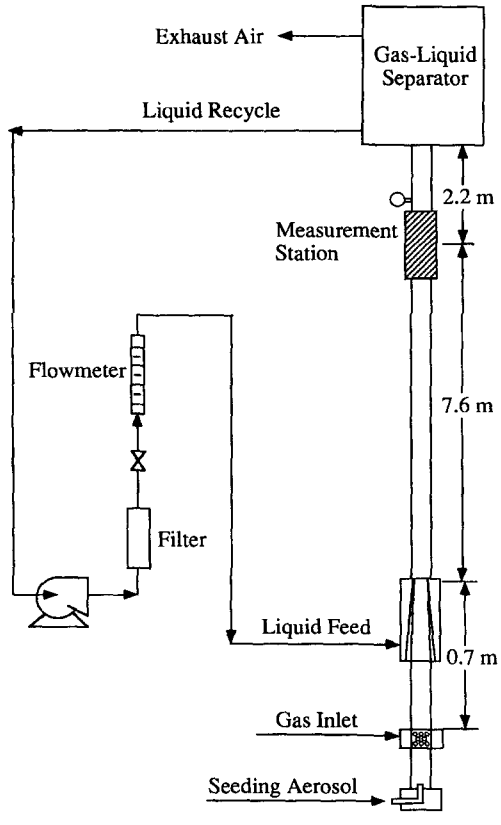

Figure 1. Multiphase flow loop.

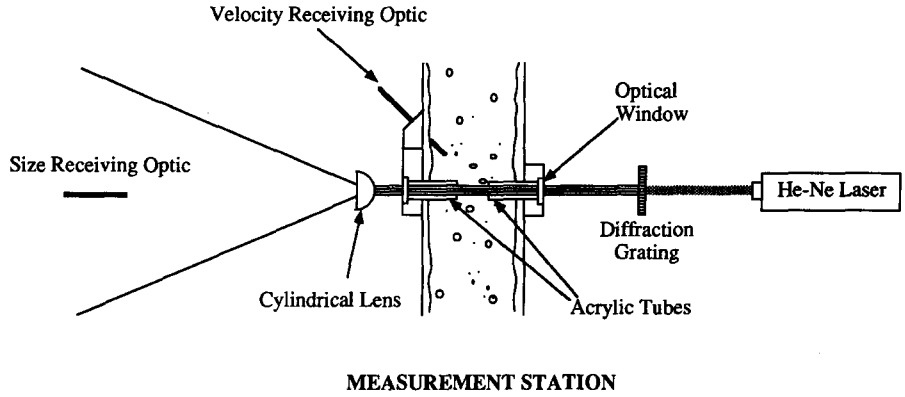

Figure 2. Experimental setup for drop size and velocity measurement.

mixtures. The liquid was introduced as a thin film by an annular–slot feed device. Air entered through a drilled acrylic section located 0.7 m below the liquid feed. During LDA measurements of the local gas velocity, an olive oil aerosol was introduced at the bottom of the column through a length of tubing. All measurements were performed at a location 7.6 m above the liquid feed, providing a flow development length of nearly 150 tube diameters.

Measurement station and techniques

The experimental setup for the simultaneous measurement of drop size and velocity is shown in figure 2. Figure 3 is an axial view of the measurement station, designed to allow access to the gas–droplet core without removal of the liquid film. A 1.3 mm dia laser beam passed through a diffraction grating and entered the tube through an optical window, attached to a 6 mm o.d. acrylic tube which penetrated the film. The receiving optic used to measure the droplet velocity was located 45° off-axis and facing the laser beam. The beam exited the station through a second window and acrylic tube, at which point it was expanded with a cylindrical lens before striking the receiving optic used for the size measurement. The size and velocity measurement occurred at the center of a 15 mm gap between the tubes. When droplets deposited on the windows, air was purged through lines integral to the acrylic tubes. Use of this measurement station assumes that the two acrylic tubes, which are necessary for access to the core, do not influence the upstream droplet size and velocity statistics. A second measurement station, with a single window extending 7 mm into the core, was used to measure the centerline gas velocity with an LDA system.

The technique for the simultaneous measurement of droplet size and velocity is essentially that described by Semiat & Dukler (1981) and extended to annular flow by Lopes & Dukler (1986). An interference pattern is created in the cross-section of a laser beam by passing it through a

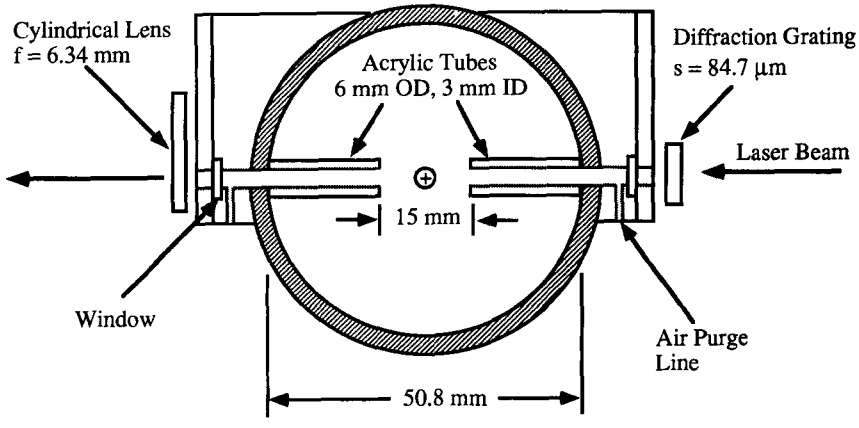

Figure 3. Axial view of measurement station.

transparent Ronchi diffraction grating. The pattern is defined by bright and dark interference fringes which are spaced identically with the lines on the diffraction grating. As a transparent droplet passes through the interference pattern, it refracts light forward so that the optic located 45° above the beam axis observes a fluctuating light intensity corresponding to the droplet's motion through successive bright and dark fringes. The velocity of the droplet, V_d, is obtained from the frequency of light fluctuation, f, and the fringe spacing, s, as

$$V_d = fs. \quad [1]$$

The sample volume for this technique is defined by the intersection of the velocity receiving the optic's line-of-sight with the 1.3 mm laser beam (Semiat & Dukler 1981). The receiving optic was a 0.9 mm dia fiber, recessed in steel tubing, so that the line-of-sight can be approximated as a 0.9 mm cylinder. The length of the intersection along the beam axis is approx. 2.6 mm in this case, larger than any of the measured drops.

As a droplet is immersed in the laser beam, it casts a shadow, reducing the intensity of light striking a fiber optic located on-axis with the beam. The passage time during which the intensity reduction takes place, T, is determined by

$$T = \frac{d + M}{V_d}, \quad [2]$$

where d is the drop size and M is the thickness of the receiving optic. The size, d, is the diameter for a spherical drop and the length of the vertical axis for a distorted drop.

The size of the fiber optic, M, in [2] is crucial to the measurement. It should be significantly smaller than the droplet for the measurement to be unbiased. The value of M in the Lopes & Dukler technique was approx. 100 μm, hence the lower limit in size resolution. This has been improved by expanding the laser beam with the cylindrical lens shown in figure 2. Within the expanded beam, the effective size of the optic is reduced proportionately. The 500:1 expansion used here reduced the effective size of a 0.9 mm fiber optic to approx. 2 μm, so that droplets as small as 10 μm were measured with confidence.

A 35 mW He–Ne laser, a diffraction grating with a line spacing of 84.7 μm and a cylindrical lens with a 6.34 mm focal length were used in the optical setup. Two photomultipliers were used to obtain the droplet velocity and size signals from optical fibers recessed in hypodermic tubing. The velocity signals were analysed with a TSI 1090 counter. A special circuit designed by Circuit Concepts, Inc. (Houston, Tex.), analyzed the passage time signals and synchronized them with the velocity signals. The gas velocity was measured with a Dantec LDA system and Burst Spectrum Analyzer (BSA). Further details of the experimental method and equipment are given by Fore (1993).

Operating conditions

Experiments were performed for air and two liquids over a range of gas and liquid flow rates. The liquids were water and a 50% glycerine–water mixture with physical properties summarized in table 1 (Miner & Dalton 1953). It is noted here that the surface tension for both liquids is essentially the same. The boundary between film-churning and upward-traveling disturbance waves occurred around gas velocities of 19 m/s. The gas flow rates cover one condition in film-churning for each liquid flow rate, with all others in the region of upward-traveling disturbance waves.

Liquid feed rates were chosen so that the two liquids could be compared on the basis of volumetric flow rate, or volumetric flow per unit perimeter, Γ. Liquid Reynolds numbers, $Re_L = 4\Gamma/\nu$ where ν is the kinematic viscosity, of 140, 280, 420 and 560 for the 6 cP liquid can thus be compared on the basis of Γ to 750, 1500, 2250 and 3000, respectively, for the 1 cP liquid.

Table 1. Properties of test liquids

	Viscosity	Density	Surface tension
1 cP liquid	1.05 cP	999 kg/m^3	72 dyn/cm
6 cP liquid	6.05 cP	1128 kg/m^3	70 dyn/cm

Table 2. Drop size statistics for the 1 cP liquid

Re_L	ρ_G (kg/m^3)	U_{GS} (m/s)	Sample size	Number mean (μm)	Surface mean (μm)	Volume mean (μm)	SMD (μm)	d_{99} (d_{max}) (μm)
750	1.18	18.1	11,874	245	307	364	519	1110
750	1.25	20.3	18,585	225	280	329	462	980
750	1.28	23.3	21,653	218	268	312	432	960
750	1.32	26.0	19,888	219	269	313	432	940
750	1.38	28.4	21,493	209	253	291	393	880
750	1.42	31.5	18,753	211	249	280	361	770
750	1.44	33.0	19,099	212	257	302	426	1080
1500	1.18	17.9	5955	286	363	431	620	1280
1500	1.25	20.2	14,295	245	311	370	533	1130
1500	1.28	23.1	17,559	239	297	348	488	1090
1500	1.32	26.0	19,784	230	284	331	460	1030
1500	1.38	28.4	19,830	216	264	306	416	910
1500	1.42	31.5	10,920	222	266	304	403	910
1500	1.44	32.4	8572	218	266	307	415	930
2250	1.18	17.6	3772	363	472	571	854	1690
2250	1.25	20.0	9334	304	385	460	668	1440
2250	1.28	23.1	11,259	282	354	420	599	1300
2250	1.32	25.9	12,789	267	331	389	546	1200
2250	1.38	28.3	10,794	255	322	388	573	1340
2250	1.42	31.2	7349	274	338	397	558	1250
2250	1.44	32.7	6041	265	325	379	526	1200
3000	1.18	17.3	2737	424	551	662	976	1760
3000	1.25	19.9	6713	377	489	590	875	1700
3000	1.28	23.0	7170	340	433	518	753	1570
3000	1.32	25.9	7780	320	409	493	728	1570
3000	1.38	28.3	5767	317	410	499	753	1570
3000	1.42	31.3	4860	318	399	475	685	1430
3000	1.44	32.1	4074	318	399	477	695	1490

MEASUREMENTS

Drop size distributions

A large number of drop size and velocity measurements were obtained for each experimental condition, ranging from 2700 to 21,000. Consequently, random errors associated with mean values,

Table 3. Drop size statistics for the 6 cP liquid

Re_L	ρ_G (kg/m^3)	U_{GS} (m/s)	Sample size	Number mean (μm)	Surface mean (μm)	Volume mean (μm)	SMD (μm)	d_{99} (d_{max}) (μm)
140	1.18	16.9	9604	303	380	454	662	1450
140	1.25	20.1	15,948	253	313	374	543	1320
140	1.28	23.2	14,150	232	278	321	435	1060
140	1.32	26.1	14,964	228	269	308	412	1040
140	1.39	28.7	11,684	229	268	310	420	1130
140	1.42	31.6	11,669	228	279	339	511	1280
280	1.18	16.6	5861	386	496	599	894	1720
280	1.25	19.9	9481	309	397	486	745	1620
280	1.28	23.2	9136	279	349	420	618	1470
280	1.32	26.0	9967	256	318	383	565	1360
280	1.39	28.6	15,879	224	275	327	470	1180
280	1.42	31.6	12,376	232	288	347	515	1260
420	1.18	16.3	5152	471	608	729	1070	1870
420	1.25	19.9	7535	378	495	608	936	1780
420	1.28	23.1	5701	362	465	567	859	1710
420	1.32	25.9	7185	335	431	527	802	1620
420	1.39	28.5	6746	310	401	494	764	1570
420	1.42	31.5	6291	305	394	487	757	1590
560	1.18	16.6	2997	507	665	793	1151	1860
560	1.25	19.5	4465	489	641	772	1139	1890
560	1.28	23.6	6344	425	558	679	1023	1830
560	1.32	25.8	5578	413	544	663	1008	1820
560	1.39	28.4	3512	390	503	612	922	1770
560	1.42	31.5	4048	380	492	600	912	1790

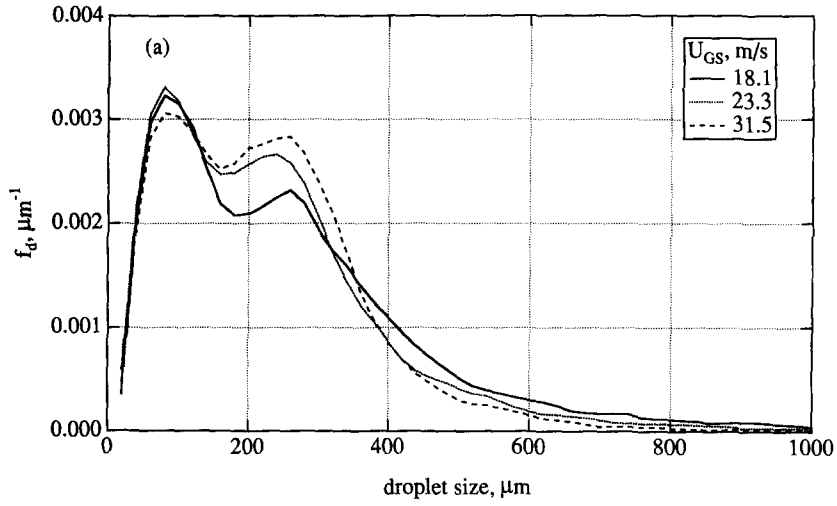

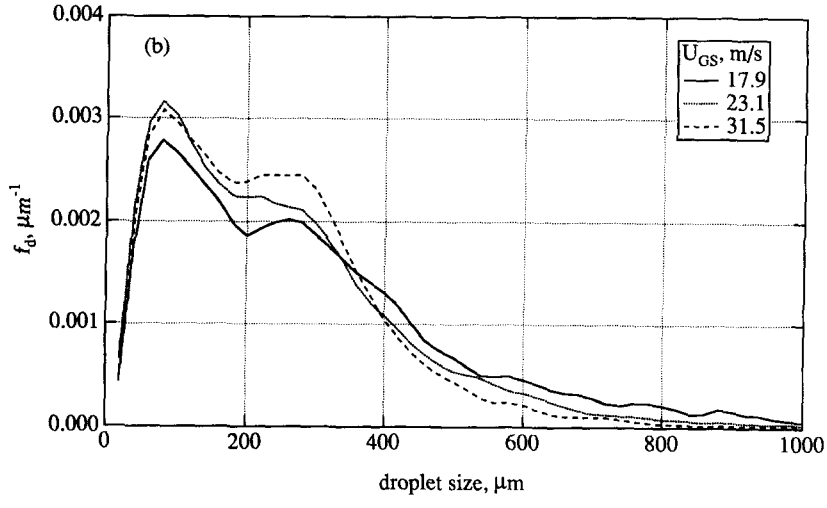

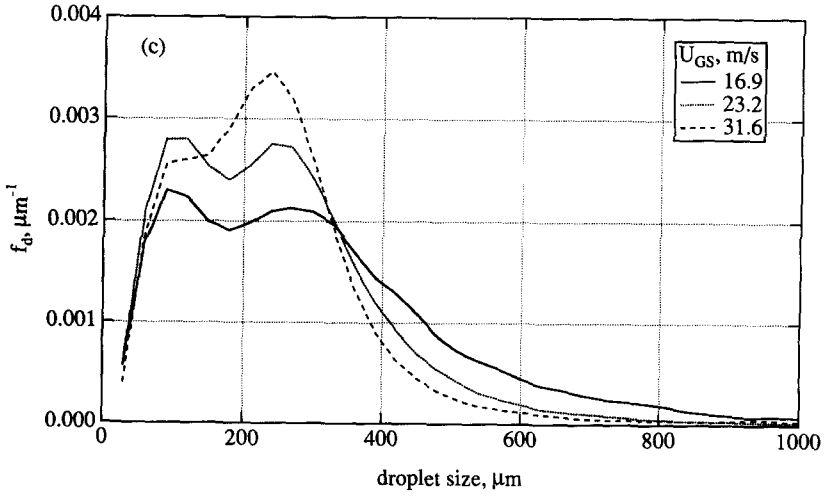

Fig. 4(a)–(c). *Caption opposite.*

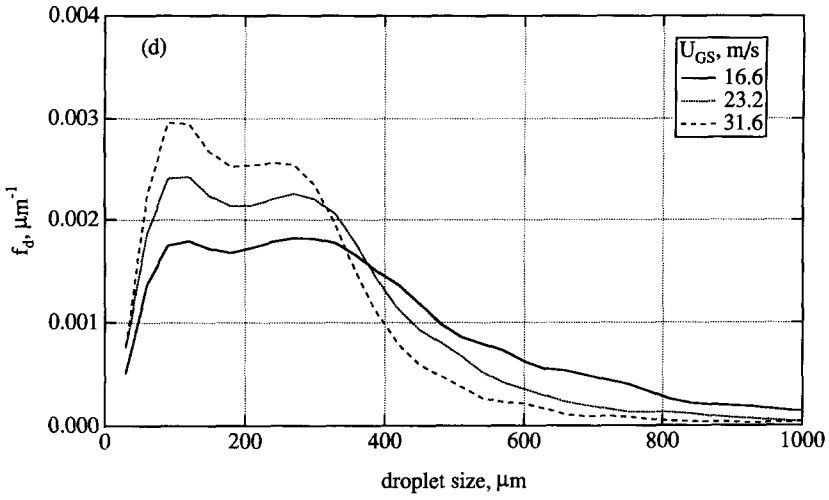

Fig. 4(d)

Figure 4. Centerline drop size probability density functions. (a) 1 cP liquid, $Re_L = 750$; (b) 1 cP liquid, $Re_L = 1500$; (c) 6 cP liquid, $Re_L = 140$; (d) 6 cP liquid, $Re_L = 280$.

and with the probability density functions (p.d.f.s), are negligibly small. Typical drop size p.d.f.s, obtained at the tube centerline, are shown in figure 4 for the two liquids. Two peaks are observed in the size distribution for these examples, as well as for measurements obtained under other conditions. The bimodal nature of these drop size distributions is more complicated than previously reported but is observed here only with the expanded size range and large number of samples. One consequence of this behavior is the discounting of previously-used single-mode functions to describe the drop size distribution in annular flow. These include the upper-limit function of Mugele & Evans (1951), which has been used by Wicks (1966), Tatterson *et al.* (1977), and Lopes (1984); and the Rosin–Rammler function, which is implicit in the laser-diffraction technique used by Azzopardi *et al.* (1978).

The characteristic maximum drop size, d_{max}, is approximated here by the 99th percentage point, d_{99}, of the size distribution. The mean drop sizes were then calculated by including all drops smaller than d_{max}. This eliminated the unrepresentative, anomalously large droplets, which can severely affect the higher-order means. Tables 2 and 3 list the number mean, area mean, volume mean, Sauter mean, and the 99th percentage point for each condition. Figure 5 illustrates the dependence of the number mean, d_{10}, on gas and liquid flow rates. The Sauter mean size, SMD, is of more interest, due to its use in mass transfer, reaction and combustion calculations. Figure 6 illustrates the dependence of the SMD on flow conditions. In general, the mean drop sizes decrease with increasing gas velocity and increase with increasing liquid flow rate and viscosity. When plotted vs the droplet concentration, C_E as in figure 7, a nearly single dependence is found for the SMD. This behavior is consistent with Azzopardi's (1985) argument that increasing the concentration should cause drops to coalesce, thus producing larger sizes.

Additional drop size measurements were performed for the 1 cP liquid at radial positions of $r = 1$ and 2 cm, referenced from the tube centerline. Figure 8 illustrates the radial distribution of the number mean drop size, d_{10}, for Reynolds numbers of 750 and 3000. At $Re_L = 750$, the mean drop size is approximately constant from the centerline to the tube wall. However, for $Re_L = 3000$, the drop size is appreciably larger at the centerline and decreases continuously to the tube wall. This behavior at the larger Reynolds number can be explained by the inertia of the larger droplets, which makes them more likely to migrate to the centerline and remain there.

Drop velocity distributions

Probability density functions for the droplet axial velocity at the tube centerline are shown in figure 9 for the 1 cP liquid. The droplet velocity distributions extend well past the superficial gas velocity, which is itself significantly lower than the mean gas velocity at the centerline. Another

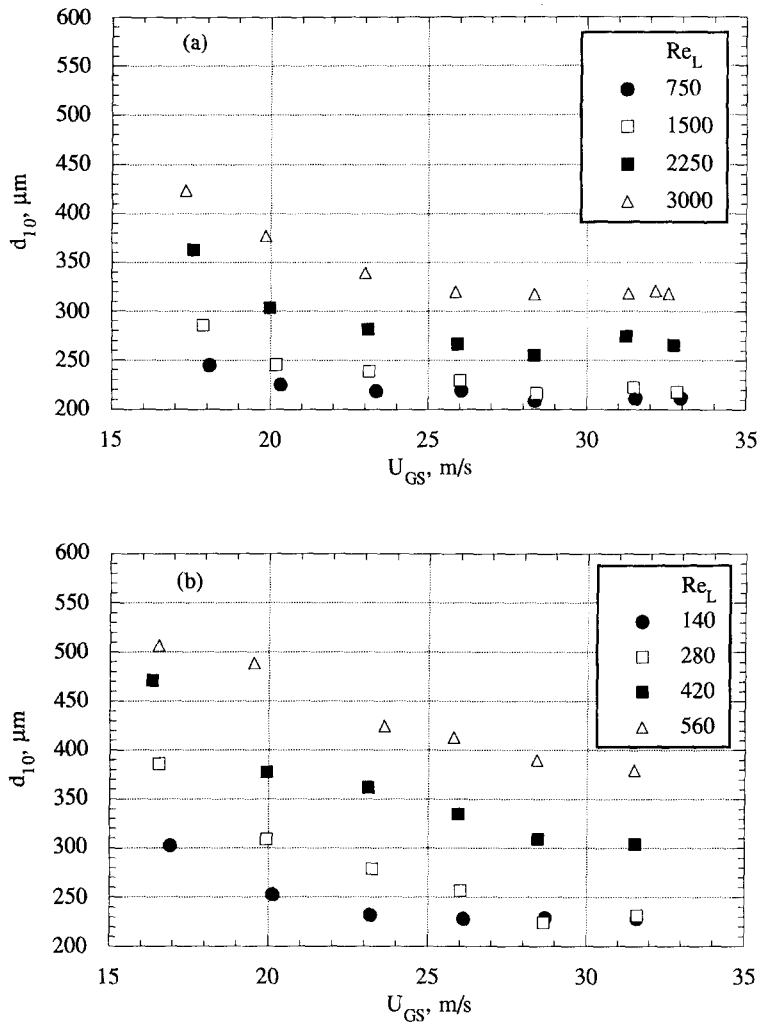

Figure 5. Number mean drop sizes; (a) 1 cP liquid; (b) 6 cP liquid.

point of interest is the increasing dispersion of the velocity distributions with increasing gas velocity. The mean droplet axial velocity for the same liquid is shown in figure 10.

Additional measurements at radial positions of $r = 1$ and 2 cm from the tube centerline were used to produce the radial profiles of drop velocity shown in figure 11 for $Re_L = 750$. These profiles are similar to the radial profiles of gas velocity, which are steeper than the flat profiles expected in a single-phase turbulent flow (Gill *et al.* 1964; Jayawardena 1993). The mean slip ratio, S_R, is defined with the droplet superficial velocity, U_D, as

$$S_R = \frac{U_D}{U_{GS}}. \qquad [3]$$

It describes the interphase slip, which is important to gas–droplet convective transport and droplet acceleration. An estimate of the droplet superficial velocity requires the radial distribution of droplet velocity, which is presented above, along with the radial concentration of droplets which was not obtained. Local measurements of the gas velocity, however, provide the slip ratio at the tube centerline, S_{R0}, defined with the mean centerline gas velocity, V_G, and the mean centerline droplet velocity as

$$S_{R0} = \frac{V}{V_G}. \qquad [4]$$

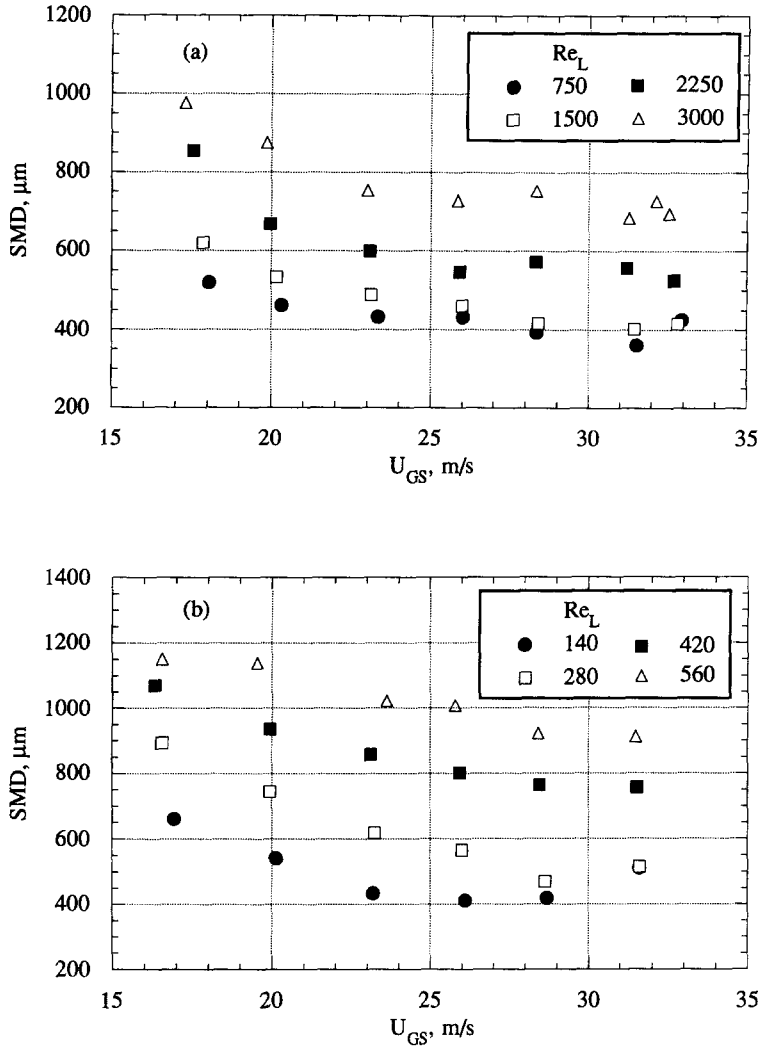

Figure 6. Sauter mean drop sizes: (a) 1 cP liquid; (b) 6 cP liquid.

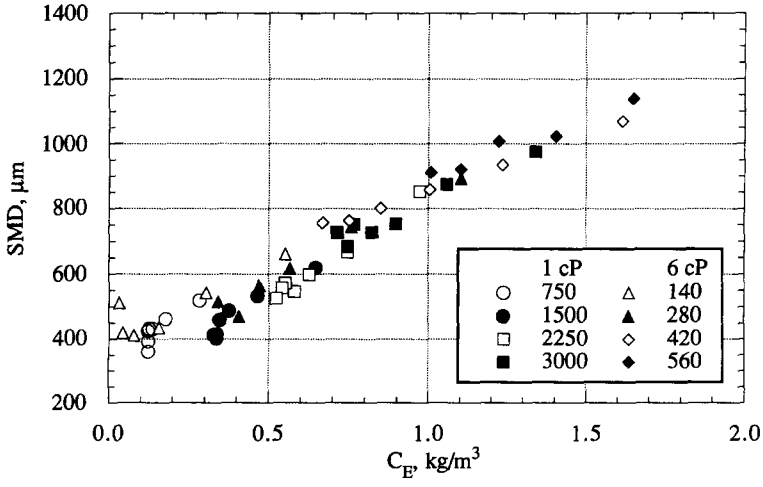

Figure 7. Dependence of Sauter mean drop size on droplet concentration.

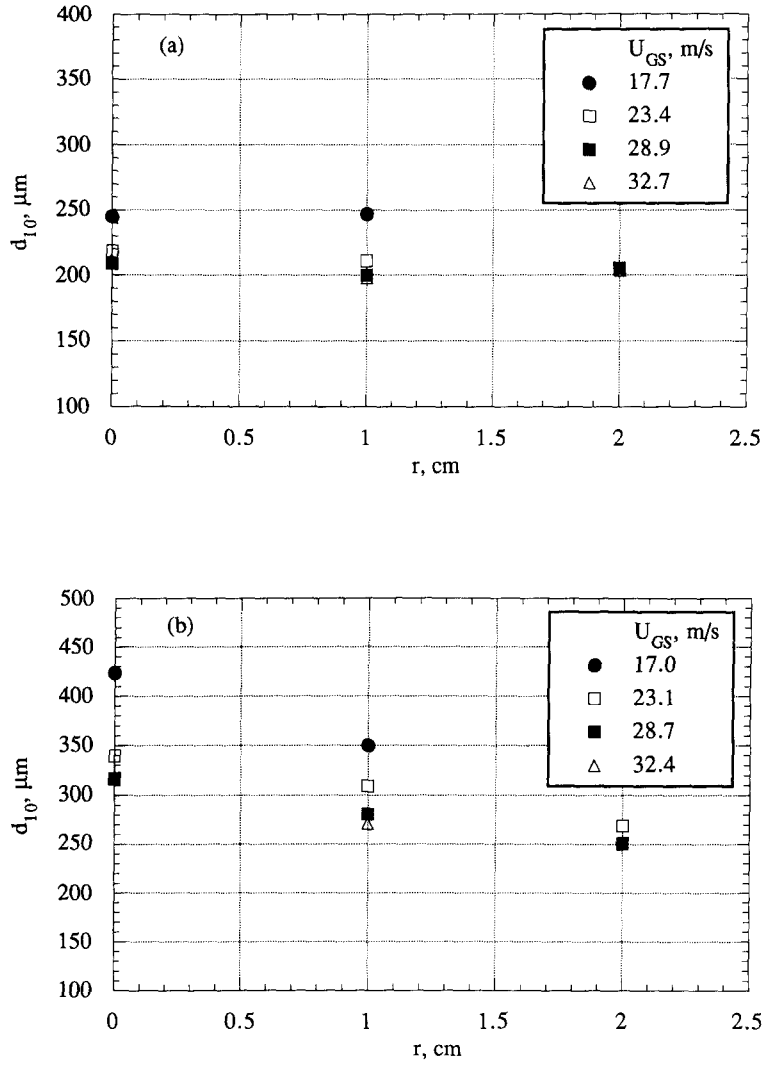

Figure 8. Radial distribution of number mean drop size for the 1 cP liquid. (a) $Re_L = 750$; (b) $Re_L = 3000$.

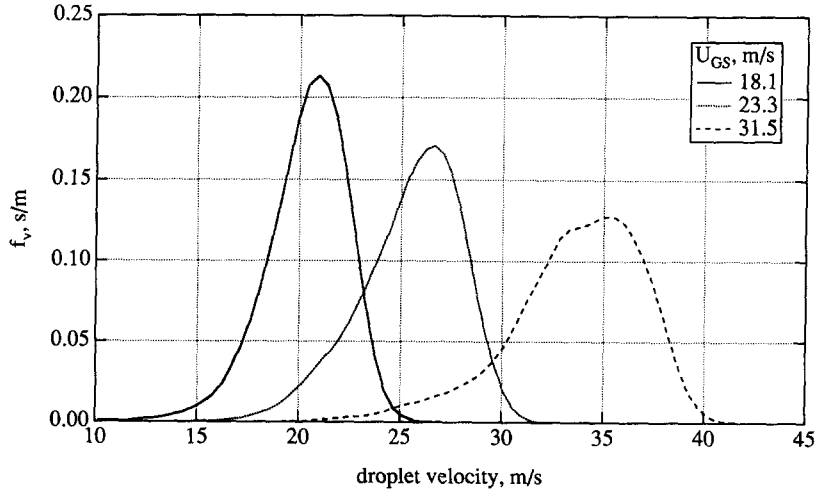

Figure 9. Drop velocity probability density functions for the 1 cP liquid at $Re_L = 750$.

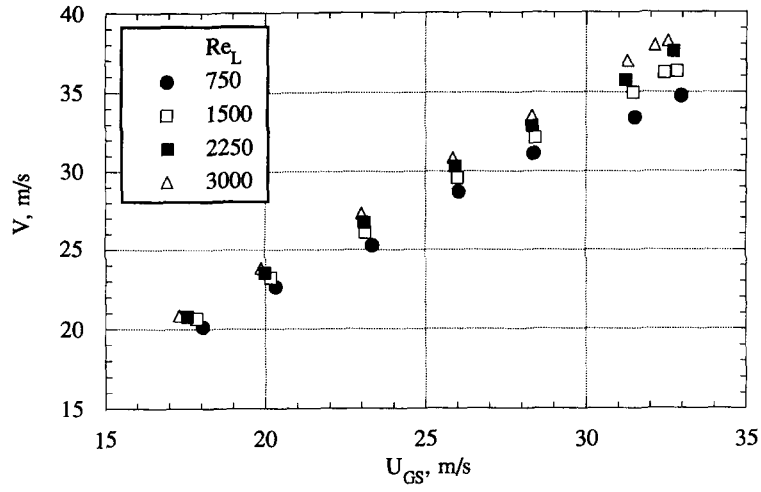

Figure 10. Mean centerline drop velocity for the 1 cP liquid.

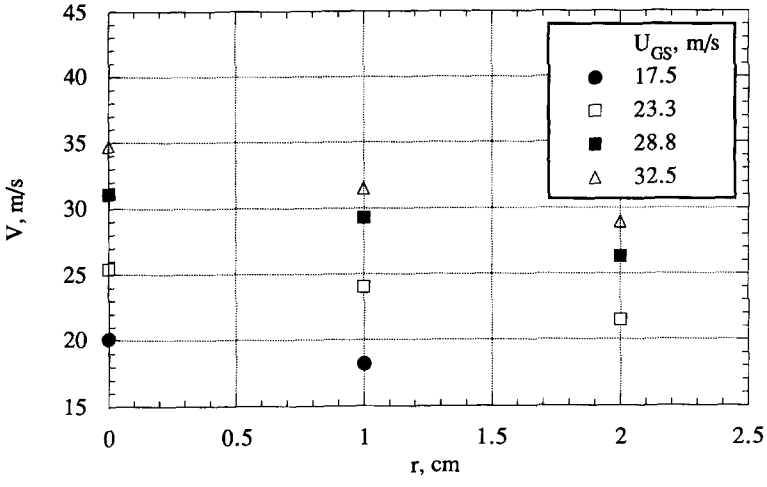

Figure 11. Radial distribution of droplet velocity for the 1 cP liquid at $Re_L = 750$.

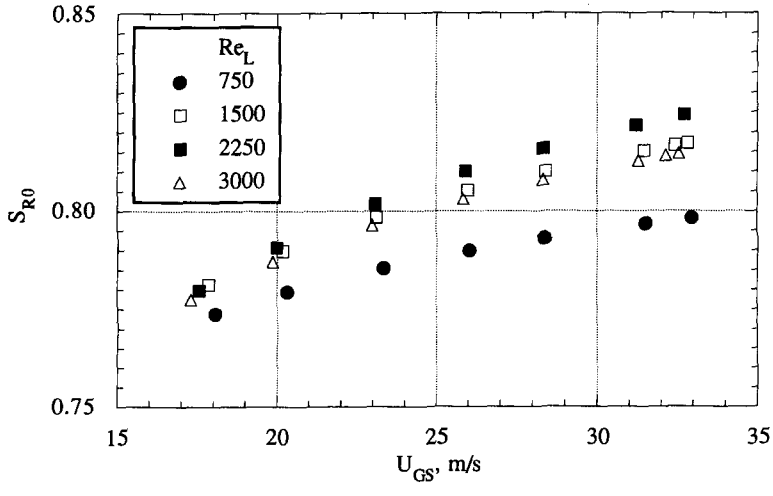

Figure 12. Centerline slip ratio for the 1 cP liquid.

Figure 12 illustrates this quantity for the 1 cP liquid. Under the present circumstances, the droplets at the centerline are traveling, on average, at 80% of the local mean gas velocity. Terminal slip ratios, as estimated from standard drag curves, are much closer to unity. This indicates that the droplets at the centerline are still undergoing acceleration, increasing the pressure drop of the system.

SUMMARY

An improved technique has been used to measure droplet size and velocity distributions in upward annular flow. The size distributions exhibit twin modes, discounting the use of previously-suggested standard functions to describe them. The mean drop sizes are dependent on liquid flow rate and viscosity, increasing with increases in both. The mean gas–droplet slip ratio is approx. 80% at the tube centerline, indicating significant axial acceleration.

Acknowledgements—This work was made possible by financial support from the Office of Naval Research, under grant N00014-90-J-1090 and the Shell Development Company.

REFERENCES

AZZOPARDI, B. J., FREEMAN, G. & WHALLEY, P. R. 1978 Drop sizes in annular two-phase flow. UKAEA Report AERE-R9074.

AZZOPARDI, B. J., FREEMAN, G. & KING, D. J. 1980 Drop sizes and deposition in annular two phase flow. UKAEA Report AERE-R9634.

AZZOPARDI, B. J. 1985 Drop sizes in annular two-phase flow. *Exp. Fluids* **3,** 53–59.

AZZOPARDI, B. J., PEARCEY, A. & JEPSON, D. M. 1991 Drop size measurements for annular two-phase flow in a 20 mm diameter vertical tube. *Exp. Fluids* **11,** 191–197.

AZZOPARDI, B. J. & TEIXIERA, J. C. F. 1992 Gas core turbulence and drop velocities in vertical annular two phase flow. *28th National Heat Transfer Conference and Exhibition*, San Diego, ASME HTD, **197,** 37–46.

BACHALO, W. D. 1980 U.S. Pat. 4540283.

COUSINS, L. B. & HEWITT, G. F. 1968 Liquid phase mass transfer in annular two phase flow: droplet deposition and liquid entrainment. UKAEA Report, AERE-R5657.

FORE, L. B. 1993 Droplet entrainment in vertical gas–liquid annular flow. Ph.D. dissertation, University of Houston.

GILL, L. E., HEWITT, G. F. & LACEY, P. M. C. 1964 Sampling probe studies of the gas core in annular flow—II: Studies of the effect of phase flow rates on phase and velocity distribution. *Chem. Engng Sci.* **19,** 665–682.

HALL-TAYLOR, N. S., HEWITT, G. F. & LACEY, P. M. C. 1963 The motion and frequency of large disturbance waves in annular two-phase flow of air–water mixtures. *Chem. Engng Sci.* **18,** 537–552.

JAYAWARDENA, I. M. S. S. 1993 Turbulent flow in the core region of vertical annular gas–liquid flow. Ph.D. dissertation, University of Houston.

JEPSON, D. M., AZZOPARDI, B. J. & WHALLEY, P. B. 1989 The effect of gas properties on drops in annular flow. *Int. J. Multiphase Flow* **15,** 327–339.

JEPSON, D. M., AZZOPARDI, B. J. & WHALLEY, P. B. 1990 The effect of physical properties on drop size in annular flow. *Proc. 9th Int. Heat Transfer Conf.*, Vol. 6, pp. 95–100.

LOPES, J. C. B. 1984 Droplet sizes, dynamics and deposition in vertical annular flow. Ph.D. dissertation, University of Houston.

LOPES, J. C. B. & DUKLER, A. E. 1986 Droplet entrainment in vertical annular flow and its contribution to momentum transfer. *AIChE Jl* **32,** 1500–1515.

LOPES, J. C. B. & DUKLER, A. E. 1987 Droplet dynamics in vertical gas–liquid annular flow. *AIChE Jl* **33,** 1013–1023.

MINER, C. S. & DALTON, N. N. 1953 *Glycerol.* Reinhold, New York.

MUGELE, R. A. & EVANS, H. D. 1951 Droplet size distribution in sprays. *Ind. Engng Chem.* **43,** 1317–1325.

NEDDERMAN, R. M. & SHEARER, C. J. 1963 The motion and frequency of large disturbance waves in annular two-phase flow of air–water mixtures. *Chem. Engng Sci.* **18,** 661–670 (1963).

SEMIAT, R. & DUKLER, A. E. 1981 Simultaneous measurement of size and velocity of bubbles or drops: A new optical technique. *AIChE J.* **27,** 148–159.

SWITHENBANK, J., BEER, J. M., TAYLOR, D. S., ABBOTT, D. & MCGREATH, G. C. 1976 A laser diagnostic technique for the measurement of droplet and particle size distributions. Paper 76-69, 14th Aerospace Sciences Meeting, Washington, AIAA.

TATTERSON, D. F., DALLMAN, J. C. & HANRATTY, T. J. 1977 Drop sizes in annular gas–liquid flows. *AIChE J.* **23,** 68–76.

WICKS, M. 1966 Liquid film structure and drop size distribution in two-phase flow. Ph.D. dissertation, University of Houston.

WICKS, M. & DUKLER, A. E. 1966 *In situ* measurements of drop size distribution in two-phase flow: A new method for electrically conducting liquids. In *Proc. 3rd Int. Heat Transfer Conf.* Vol. 5, pp. 39–48.